Self-Assembly of Bottlebrush-Linear, Rod-Coil Copolymers into Discoidal Nanoparticles

Simran D. Kerai,[a] Shin Takano,[a] Ping Zeng,[a] Markus Müllner[a,b]*

[a] Key Centre for Polymers & Colloids, School of Chemistry, The University of Sydney, Sydney NSW 2006, Australia.

[b] The University of Sydney Nano Institute, Sydney NSW 2006, Australia.

Table of Contents graph

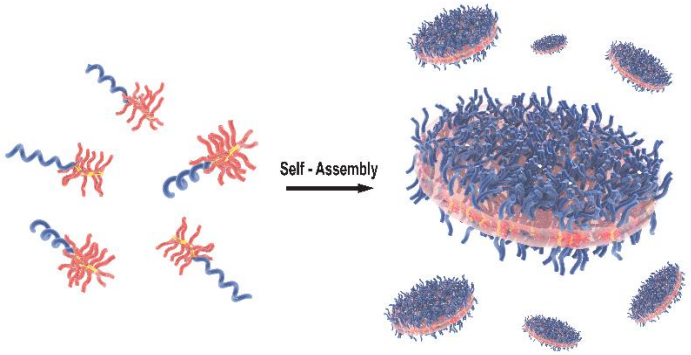

ABSTRACT: Block copolymers can self-assemble into nanoscale objects with various morphologies, offering custom nanomaterials for diverse fields of application. However, achieving amorphous 2D morphology through self-assembly in solution remains challenging. Here, we systematically investigate the structural requirements of rod (bottlebrush) – coil (linear) block copolymers for self-assembly into nanoscale discs by independently varying sidechain and backbone lengths. We identify optimal polymer dimensions that yield well-defined nanodiscs with 50-200 nm diameters through direct self-assembly in water.

Polymeric nanoparticles have revolutionized fields such as electronics, materials science and nanotechnology.[1] Especially, anisotropic particles, like discoidal nanoparticles, exhibit distinct advantages in applications requiring controlled surface interactions and tailored mechanical properties.[2, 3] Their large surface area and unique 2D geometry enhance interfacial behaviour and dispersion stability.[4, 5] Their high aspect ratio introduces atypical flow behaviour in fluids that influence particle alignment and aggregation.[6-8] We have recently summarized the development of nanodisc fabrication techniques, which remain considerably scarce compared to other polymer particle morphologies, like spheres and worms.[9] This is attributed to the significant challenge of overcoming energetic penalties that favor curved interfaces and inhibit the formation and stabilization of planar structures like discs. In this context, the use of crystallization to achieve planar 2D copolymer assemblies has emerged; initially through the crystallization of micelle cores, nowadays predominately through the growth of polymer platelets using crystallization-driven self-assembly (CDSA).[10] Thus, the fabrication of discoidal nanoparticles with crystalline cores has become controllable and reliable. In the absence of crystalline polymers, the

challenge of fabricating amorphous, discoidal nanoparticles remains. Rod-coil architectures involving linear polymers, attached to helical[11, 12] or polypeptide segments,[13-15] demonstrate the ability to form discoidal structures as their rod segments facilitate planar packing.[16] However, in either case – CDSA or linear rod-coil copolymers – the core of the assembled particles is densely packed and essential for particle stability which may hamper future applications where access to the core is important, like in drug delivery. In an effort to use non-crystalline polymers in self-assembly, approaches exploring external stimuli,[17-19] templates[20] or small molecules[21, 22] as driving forces have been studied. The complexity of these approaches underscores the necessity to develop more generalized methodologies that enable 2D assembly and that can be applied across different polymer systems and application contexts.

A modular direct self-assembly into discoidal nanoparticles can be achieved using a molecular polymer bottlebrush system, where the bottlebrush adopts the properties of a rod segment like in linear rod-coil copolymers. Chen and coworkers showed 2D self-assembly of discs using rod-coil copolymers, approximating ~400 nm in width and ~30 nm in height, using strong π-π stacking within the core-forming rods.[23] We have recently demonstrated self-assembly of a functional linear-*block*-bottlebrush copolymer 'tadpole' into discs ranging between 300 – 500 nm in diameter.[24] We further demonstrated the modularity of this approach by varying the hydrophobicity of the core-forming bottlebrush, revealing that different sidechains can be grafted without compromising the disc formation process.[25] To expand our understanding of disc-forming building blocks, we herein show that a more modular 'grafting-from' approach is advantageous in designing building blocks for nanodiscs self-assembly, as it allows to systematically identify an optimal window where nanodiscs can be realized. Similarly, we show that bottlebrushes with high glass transition temperature (T_g) can also form well-defined nanodiscs, similar to their low T_g analogues.

Scheme 1. Synthesis of PEG-*b*-(PBIEM$_x$-*g*-PBzMA$_y$) tadpole-like rod-coil bottlebrush copolymers.

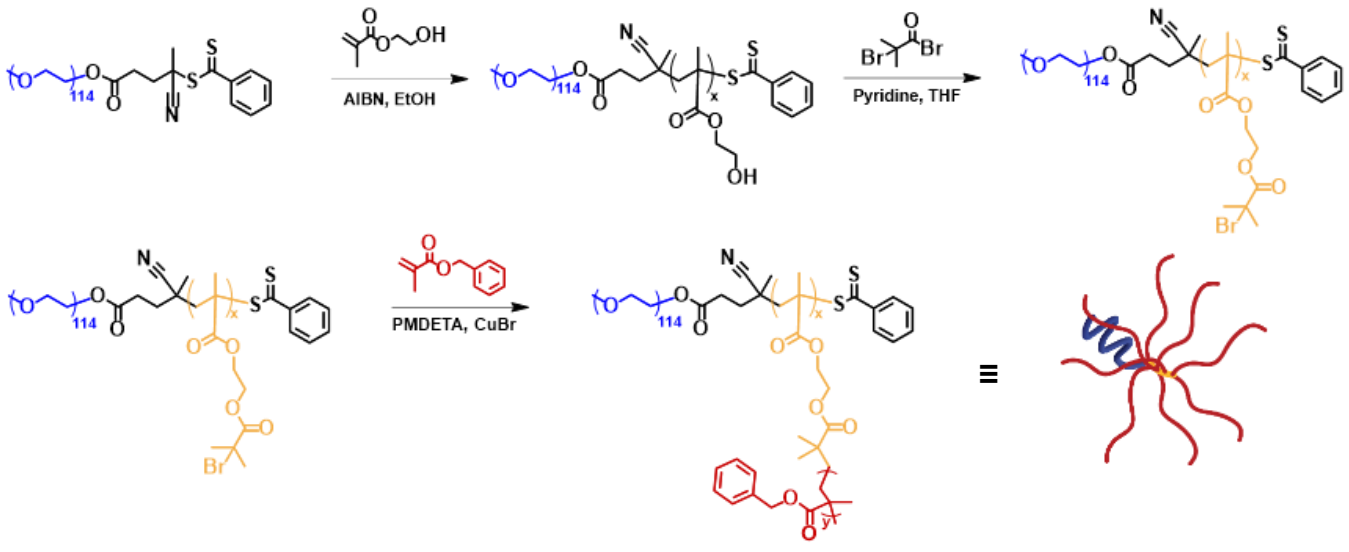

footnote: x = 9, 15, 31, 49 and y = 6, 23, 51, 75, 144

Inspired by our tadpole-like, rod-coil bottlebrush copolymers (BBCPs) made via the "grafting-to" approach,[24, 25] we designed a "grafting-from" strategy to build a library of amphiphilic BBCPs using a linear PEO block (coil) and a poly(benzyl methacrylate) (PBzMA) bottlebrush block (rod) (Scheme 1). First, we used reversible addition-fragmentation chain-transfer (RAFT) polymerization to synthesize a diblock copolymer by polymerizing 2-hydroxyethyl methacrylate (HEMA) from a $mPEG_{114}$-CPADB macro-RAFT agent (Figure S1). The PHEMA was subsequently esterified with α-bromoisobutyrate bromide to give a poly(ethylene glycol)$_{114}$-*block*-poly[2-(2-bromo isobutyryloxy)ethyl methacrylate]$_x$ (PEG_{114}-*b*-$PBIEM_x$) polyinitiator backbone (Figure S2). The PBIEM moieties were then used to graft PBzMA sidechains using atom transfer radical polymerisation (ATRP) to yield well-defined tadpole-like BBCPs macromolecules. Varying the PHEMA block length and/or the PBzMA sidechain length allowed for adjusting the bottlebrush segment, and consequently the overall BBCP dimensions and hydrophilic-to-hydrophobic ratio (Table 1). As a first set, we used a PEG_{114}-*b*-$PBIEM_{15}$ backbone to generate a library of building blocks with constant backbone length, but different sidechain lengths: PEG_{114}-*b*-($PBIEM_{15}$-*g*-$PBzMA_y$), with y = 6, 23, 51, 75, 144. The growing sidechain length increased the overall hydrodynamic volume of the BBCPs, evident through a progressive shift towards shorter retention times in size exclusion chromatography (SEC) (Figure 1A). In addition, we synthesized a second BBCP set, maintaining a comparable sidechain length (DP~ 76-79), but varying the PBIEM backbone length (x = 9, 31, 49). Again, a shift in SEC retention time was attributed to the increasing hydrodynamic volume with increasing bottlebrush blocks (Figure 1B). Sidechain lengths were determined by comparison of the integration of the CH_2 of the benzyl group at δ ~ 4.75 ppm to the repeating $(CH_2)_2$ PEG signal at δ ~ 3.55 ppm (Figures S3 & S4) under the assumption of 50% grafting efficiency.[26, 27] Figure 1C shows a representative ^{1}H NMR of PEG_{114}-*b*-($PBIEM_x$-*g*-$PBzMA_y$). A summary of the BBCP libraries is shown in Table 1. From here on, we denote our materials as tadpoles (TP), encoding the DP of PBIEM backbone and the DP of the sidechains, e.g. PEG_{114}-*b*-($PBIEM_{15}$-*g*-$PBzMA_{75}$) becomes $TP_{15\text{-}75}$. All synthesis protocols are detailed in the Supporting Information.

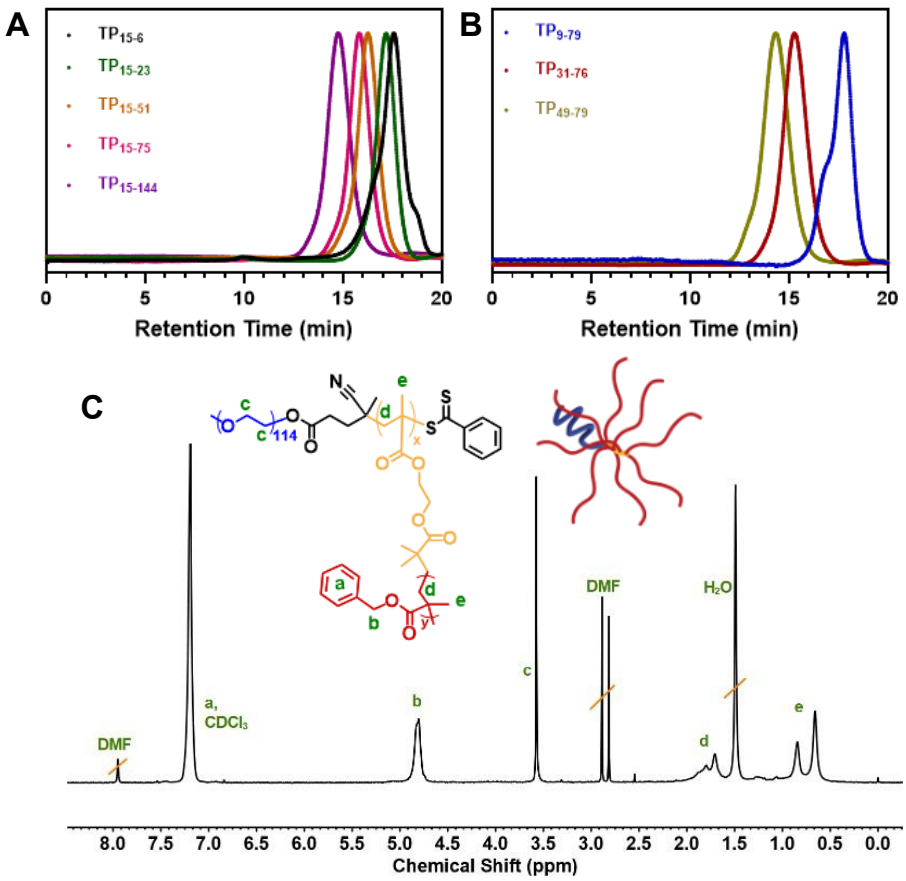

Figure 1. SEC traces in DMAc (50 °C and 1 mL min^{-1}) of (A) PEG_{114}-*b*-($PBIEM_{15}$-*g*-$PBzMA_y$) library with increasing sidechain length (y = 6, 23, 51, 75, 144) and (B) PEG_{114}-*b*-($PBIEM_x$-*g*-$PBzMA_{75}$) library with varied backbone length (x = 9, 31, 79). (C) Exemplar ^1H NMR spectrum of PEG_{114}-*b*-($PBIEM_x$-*g*-$PBzMA_y$) in $CDCl_3$.

Table 1. Characterisation data of PEG_{114}-*b*-($PBIEM_x$-*g*-$PBzMA_y$) copolymer library

BBCPs	DP_{PEG}	DP_{PBIEM}	DP_{PBzMA}	$^af_{BzMA}$	$^bM_{n,NMR}$	$^cĐ_{SEC}$	Self-Assembly Morphology
TP_{15-6}	114	15	6	0.44	12 900	1.19	Polymersomes
TP_{15-23}	114	15	23	0.75	30 400	1.11	Spherical particles
TP_{15-51}	114	15	51	0.87	72 400	1.11	Spherical particles
TP_{15-75}	114	15	75	0.91	104 000	1.11	Discs
TP_{15-144}	114	15	144	0.95	195 000	1.11	Spherical particles
TP_{9-79}	114	9	79	0.86	67 600	1.16	Polymersomes
TP_{30-76}	114	31	76	0.95	207 000	1.12	Spherical particles
TP_{45-79}	114	49	79	0.97	346 000	1.15	Spherical particles

[a]BzMA fraction in the copolymer, [b]Determined by ^1H NMR analysis, [c]Determined by SEC (M_w/M_n).

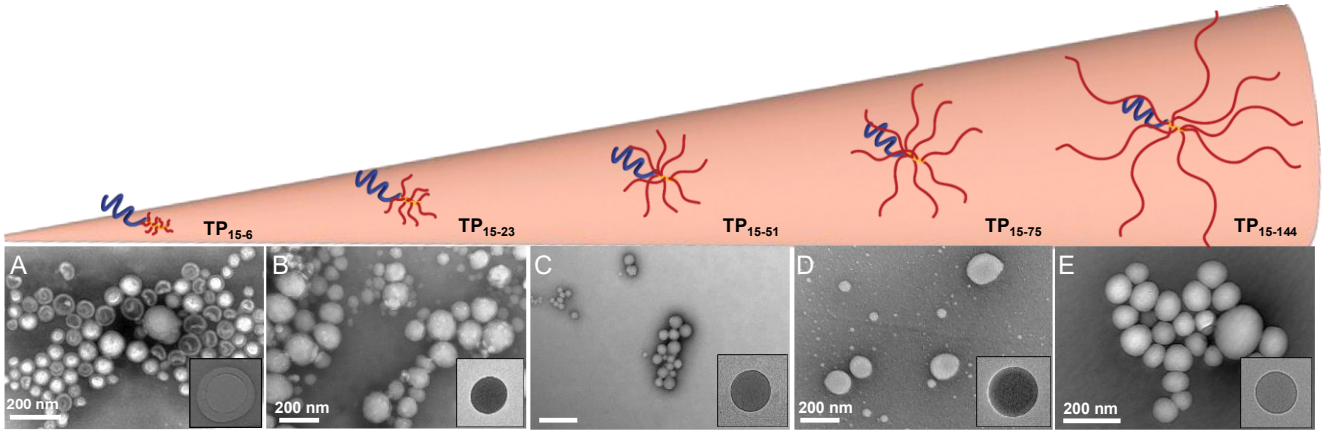

Figure 2. (top) Schematic representation of varying sidechain lengths of BBCPs with TEM images of self-assemblies from (A) $TP_{15\text{-}6}$, (B) $TP_{15\text{-}23}$, (C) $TP_{15\text{-}51}$, (D) $TP_{15\text{-}75}$, (E) $TP_{15\text{-}144}$. (bottom) TEM micrographs of negatively-stained self-assembled BBCPs, with inset showing a representative unstained particle. A schematic for each particle is provided in the Supporting Information (Figure S6).

Using the first set of BBCPs (constant PBIEM, but varying sidechain length), we self-assembled the BBCPs via a solvent switch method, starting with a 2 mg/mL solution in DMF and their dialysis into deionized water (see Supporting Information). We used transmission electron microscopy (TEM) to survey the resulting assemblies (Figure 2) and dynamic light scattering (DLS) to estimate their hydrodynamic sizes (Figure S5). The self-assembly of $TP_{15\text{-}6}$ resulted in the formation of polymersomes, as verified by TEM (Figure 2A) and AFM (Figure S7). Doubling the sidechain length in $TP_{15\text{-}23}$ revealed spherical particles averaging 200 nm in hydrodynamic diameter (Figure S5) and particles ranging from ~90-200 nm via TEM (Figure 2B). These particles were verified by atomic force microscopy (AFM), with deflated heights of ~12-28 nm indicating dense spherical particles (Figure S8). Extending sidechains further in $TP_{15\text{-}51}$ gave similar spherical morphologies, albeit with larger diameters (~80-300 nm) in TEM, AFM (Figure 2C, Figure S9) and DLS (Figure S5). Using AFM, we established that this sample also contained flat assemblies (height ~ 5 nm) that were dispersed amongst the larger spherical particles (with heights of ~20-30 nm) (Figure S9B-D). The flat particles indicated the coexistence of another species, most likely discoidal assemblies. Interestingly, when extending the sidechains further, $TP_{15\text{-}75}$ self-assembled exclusively into nanodiscs with diameters ranging from ~50-160 nm. These flat particles were observed to be uniformly shaded in TEM (Figure 2D), which aligns with previous work.[9, 24, 25] The discoidal morphology was confirmed by AFM cross-section analyses (Figure 3), which occasionally revealed stacked discs (with doubled height) amongst single discs (Figure 3B & 3C) as an artefact of the sample preparation process. As the approximate carbon-carbon length in polymethacrylates correlates to ~ 0.25 nm,[28] a stretched bottlebrush backbone would measure ~ 4-5 nm in height, indicating the BBCPs should stack side-by-side rather than end-to-end. Further extending the sidechain length, $TP_{15\text{-}144}$ resulted in the formation of spherical particles with ~ 100-200 nm diameters with deflated heights between ~25-33 nm (Figure 2E, Figure S10).

Considering the ratio of hydrophilic PEG to hydrophobic PBzMA and their macromolecular topology, we postulate that the shortest PBzMA sidechains (DP=6), combined with a reduced grafting density (ie. not 100% grafting efficiency) afford sufficient mobility of

the bottlebrush segment to be stabilised sufficiently by the hydrophilic PEG block (f_{BzMA} = 0.44, Table 1), hence leading to polymersomes. With increasing sidechain lengths, architectural asymmetry becomes more prominent relative to the flexible linear PEG, whilst increasing the hydrophobic fraction. This leads to the self-assembly of dense polymer particles, as we have recently shown for a different system.[29] Further extension of sidechain length with the grafting density remaining constant, increases crowding and steric repulsion in the bottlebrush segment, leading to segment stiffening.[30] This is further supported by theoretical predictions.[31] In addition, a strong rigidity contrast of segments in rod-coil macromolecules can diminish the influence of volume fractions and dominate thermodynamic factors in the self-assembly of discrete nanostructures.[16] At f_{BzMA} = 0.91 found in $TP_{15\text{-}75}$, this steric repulsion affects the ability of the bottlebrush segment to bend and to adopt curvature[32] during dialysis, leading to planar, discoidal assemblies. This segment stiffening is expected to be minimally affected by the nature of the solvent, provided the solvent is a good solvent for the bottlebrush. Using THF instead of DMF for the dialysis yielded also exclusively nanodiscs (Figure S14), indicating that the self-assembly depends more on the rod-coil structure than solvent effects. This aligns with molecular dynamic simulations, indicating that increasing sidechain length leads to stiffening and an extension effect on bottlebrush backbones.[33] As the ratio of PEG to PBzMA diverts further, sufficient stabilisation of the self-assembled materials becomes problematic, leading to the formation of dense polymer particles (likely large compound micelles or nanoprecipitates)[34] with low colloidal stability. Scattering experiments indicate that the flexibility of bottlebrush backbones can be restored by excessive elongation of sidechains as their mutual interaction and conformational entropy overwhelms steric effects.[35]

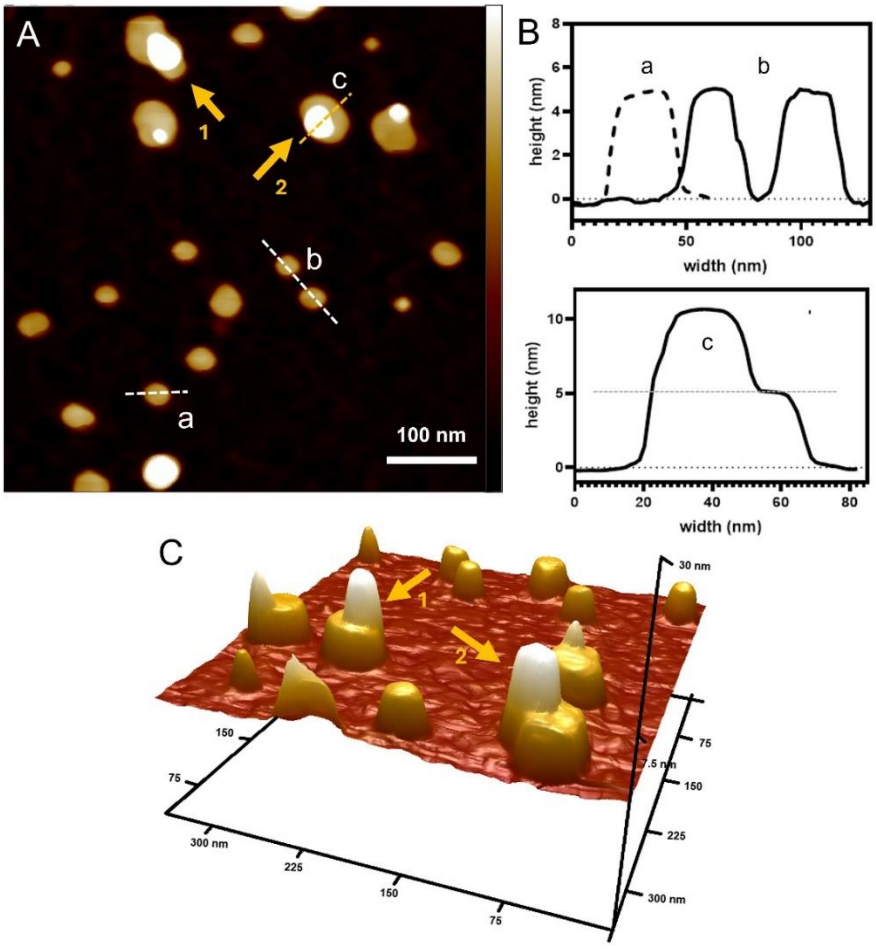

Figure 3. (A) AFM height image of self-assembled discs of $TP_{15\text{-}75}$ and its crosssectional analysis (B). (C) 3D plot of the marked section in the height image, with arrows indicating stacked discs. Z-value -1 – +7nm.

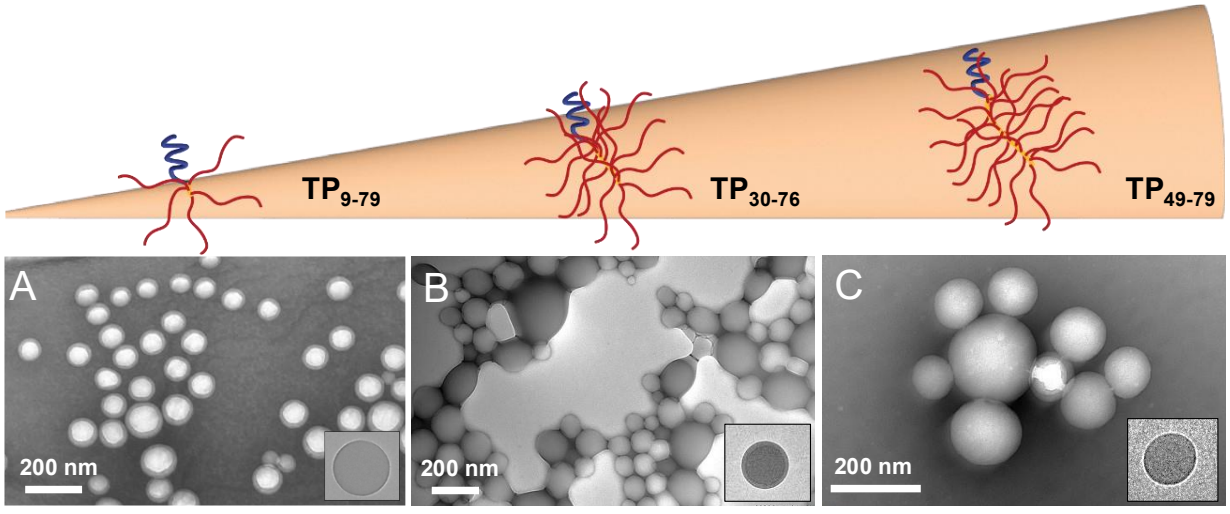

Figure 4. Schematic representation of backbone length of polymer tadpoles with (A-C) TEM images of self-assemblies from (A) $TP_{9\text{-}79}$, (B) $TP_{30\text{-}76}$, (C) $TP_{49\text{-}79}$. Scale bars are 200 nm. A schematic for each particle is provided in the Supporting Information (Figure S6).

After finding that $TP_{15\text{-}75}$ yielded polymer nanodiscs, we then varied the bottlebrush backbone length as another parameter to alter both the molar ratio and dimensions of the hydrophobic segment. Whilst the grafting density across our systems remains constant as the synthetic procedure is identical, a very short backbone length (DP = 9) in $TP_{9\text{-}79}$ will allow for less protruding sidechains and a reduced steric hindrance between the sidechains, mimicking systems with sparsely grafted sidechains.[36] Additionally, simulation studies show that shorter end-to-end backbone distances improve side chain mobility to spherically cap bottlebrush segments.[37, 38] Thus, the corresponding self-assemblies of the highly asymmetric amphiphile $TP_{9\text{-}79}$ formed polymersomes (Figure 4A, Figure S11). Despite maintaining a comparable PEG-to-PBzMA ratio in $TP_{9\text{-}79}$ (f_{BzMA} = 0.86) to $TP_{15\text{-}75}$, the curvature effect at the interface between the domains is influenced by the greater sidechain flexibility and reduced persistent length of the backbone[39] lending to vesicular structures. Increasing the backbone length in $TP_{30\text{-}76}$ and $TP_{49\text{-}79}$ meant that the hydrophobic bottlebrush segment increased dramatically in volume and was more likely to behave like a bottlebrush again due to increased chain crowding and axial backbone stretching.[38, 40] However, this resulted in the formation of spherical polymer self-assemblies (Figure 4B and 4C; Figure S12 and S13), as a result of the high hydrophobic content (f_{BzMA} > 0.95) and the reduced solubility and enhanced collapse of the bottlebrush blocks, as recently seen for a different system.[29] Whilst the increase in backbone length is expected to increase the persistence length and rigidity of the brush segment, and thus satisfy the expected requirements of planar packing, the sharp increase of the BzMA fraction ultimately leads to spherical polymer particles.

To deduce influencing parameters on disc formation, we compared the linear-to-bottlebrush molar ratios of $TP_{15\text{-}75}$ (Table 1) with that of our previously reported "grafting-to" studies using poly(ethyl glycoxylate) ($f_{hydrophobic}$ = 0.87)[24] and poly(glycidyl ether)s ($f_{hydrophobic}$ ~ 0.80)[25] sidechains. Both exhibited similar, but not matching, ratios to the disc-forming $TP_{15\text{-}75}$ ($f_{hydrophobic}$ = 0.91). However, because the chemical identity and grafting density of the hydrophobic bottlebrush segments differ across these three systems, we can expect that the critical ratio between the hydrophilic coil to the hydrophobic rod segment to facilitate planar packing will differ too. But in all these cases the bottlebrush backbone must be appropriately extended by sufficiently long sidechains that protrude from the backbone in response to steric repulsion.[32, 38] This reduces the flexibility within the core-forming segment in all cases, whilst enhancing the segregation strength between the domains of the amphiphile,[41, 42] both favorable for planar packing. Comparing the grafting densities of our grafting-from approach (~ 50%) to our grafting-to approach (~75%), it is expected that an increase in grafting density introduced sidechain overlapping and crowding more readily,[43] which in turn positively influences a persistent rigid conformation of the backbone.[40, 44] Given this depends on also on the nature of the polymer sidechains, there will be a critical sidechain length for individual disc-forming systems with sufficiently high grafting efficiency.[45] Moreover, any differences in sidechain chemical compositions (particularly the T_g) may affect the bottlebrush conformational flexibility in the self-assembly process.[46] Comparing the high T_g PBzMA[47] sidechains in this study to low T_g poly(ethyl glycoxylate)[48] and poly(glycidyl ether)s,[49] it seems that T_g has limited effect on the overall disc formation, but may affect the overall diameter of particles but due to differing sidechain mobility. Moreover,

solvent quality, provided it remains a good solvent to the polymer, seemed to minimally influence the formation process, but presents an opportunity to influence disc sizes.

In conclusion, this study revealed that a library of tadpole-like amphiphiles can be readily produced *via* a modular 'grafting-from' approach. Depending on their composition, topology and overall amphiphilic character, these amphiphiles self-assembled into either polymersomes, spherical polymer particles or nanodiscs. The window to exclusively assemble these BBCPs into nanoscale polymer discs was narrow but it demonstrated the opportunity of custom-designing building blocks with rod-coil character to produce pure polymer nanodiscs. In addition, we could demonstrate that BBCPs with a high T_g bottlebrush segment are able to form nanodiscs, just like their low T_g counterparts in previous studies. Insights from this study will aid the development of amorphous 2D nanoparticles and provide a route towards designing suitable building blocks for bottom-up fabrication of nanodiscs via solution self-assembly. While the complete mechanism of the disc formation remains unclear at this point, the above insights will aid future experiments to study the self-assembly process of rod-coil copolymers during dialysis. Previous work on rod-coil copolymers,[50] including our nanodiscs,[24] support a fusion driven self-assembly process involving intermediate assemblies. Simulation of this process will further provide understanding on bottlebrush properties in a progressively changing solvent environment. More generally, architectural asymmetry in copolymers has become a growing focus in polymer self-assembly, both experimentally and theoretically,[51-57] to which this work will contribute.

ASSOCIATED CONTENT

Full experimental and additional characterization of polymers and self-assembled particles by ^{1}H NMR, SEC, TEM, DLS and AFM. This material is available free of charge via the Internet at http://pubs.acs.org.

AUTHOR INFORMATION

Corresponding Author

* Markus Müllner, markus.muellner@sydney.edu.au

Author Contributions

S.D.K. designed and performed all experiments and AFM measurements. S.T. and P.Z. performed the TEM measurements. M.M. conceived the idea and supervised the project. The manuscript was jointly written by S.D.K. and M.M. with input from all co-authors.

Notes

The authors declare no competing financial interest.

ACKNOWLEDGMENT

This project is funded through an Australian Research Council Future Fellowship (FT200100185). This research was facilitated by access to Sydney Analytical, a core research facility at the University of Sydney. The authors acknowledge the technical and scientific assistance from Sydney Microscopy & Microanalysis, The University of Sydney node of Microscopy Australia. The authors thank Prof. Chiara Neto for providing access to atomic force microscopes and the Key Centre for Polymers and Colloids (KCPC) for access to equipment. S.D.K. is a recipient of an Australian Government RTP scholarship. S.T acknowledges The Research Fellow of Japan Society for the Promotion of Science (23KJ1862). P.Z. is supported by the USyd IPRS scheme. M.M. further acknowledges the Australian Research Council for a Discovery Project (DP220100452). M.M. is a grateful recipient of a University of Sydney Research Accelerator (SOAR) Prize and a Global Science and Technology Diplomacy Fund (GSTDS000001 – 6) grant.

REFERENCES

(1) Harish, V.; Ansari, M. M.; Tewari, D.; Yadav, A. B.; Sharma, N.; Bawarig, S.; García-Betancourt, M.-L.; Karatutlu, A.; Bechelany, M.; Barhoum, A. Cutting-edge advances in tailoring size, shape, and functionality of nanoparticles and nanostructures: A review. *Journal of the Taiwan Institute of Chemical Engineers* **2023**, *149*, 105010. DOI: https://doi.org/10.1016/j.jtice.2023.105010.

(2) Pearce, A. K.; Wilks, T. R.; Arno, M. C.; O'Reilly, R. K. Synthesis and applications of anisotropic nanoparticles with precisely defined dimensions. *Nature Reviews Chemistry* **2021**, *5* (1), 21-45. DOI: 10.1038/s41570-020-00232-7.

(3) Zhu, H.; Li, M.; Liu, B. Anisotropic Colloidal Particles by Molecular Self-Assembly: Synthesis and Application. *ChemNanoMat* **2024**, *10* (3). DOI: 10.1002/cnma.202300475.

(4) Cook, A. B.; Schlich, M.; Manghnani, P. N.; Moore, T. L.; Decuzzi, P.; Palange, A. L. Size effects of discoidal <scp>PLGA</scp> nanoconstructs in Pickering emulsion stabilization. *Journal of Polymer Science* **2022**, *60* (9), 1480-1491. DOI: 10.1002/pol.20210748.

(5) Ballard, N.; Law, A. D.; Bon, S. A. F. Colloidal particles at fluid interfaces: behaviour of isolated particles. *Soft Matter* **2019**, *15* (6), 1186-1199. DOI: 10.1039/c8sm02048e.

(6) Gimondi, S.; Ferreira, H.; Reis, R. L.; Neves, N. M. Microfluidic Devices: A Tool for Nanoparticle Synthesis and Performance Evaluation. *ACS Nano* **2023**, *17* (15), 14205-14228. DOI: 10.1021/acsnano.3c01117.

(7) Doshi, N.; Prabhakarpandian, B.; Rea-Ramsey, A.; Pant, K.; Sundaram, S.; Mitragotri, S. Flow and adhesion of drug carriers in blood vessels depend on their shape: A study using model synthetic microvascular networks. *Journal of Controlled Release* **2010**, *146* (2), 196-200. DOI: 10.1016/j.jconrel.2010.04.007.

(8) Blanco, E.; Shen, H.; Ferrari, M. Principles of nanoparticle design for overcoming biological barriers to drug delivery. *Nature Biotechnology* **2015**, *33* (9), 941-951. DOI: 10.1038/nbt.3330.

(9) Brisson, E. R. L.; Worthington, M. J. H.; Kerai, S.; Müllner, M. Nanoscale polymer discs, toroids and platelets: a survey of their syntheses and potential applications. *Chemical Society Reviews* **2024**, *53* (4), 1984-2021. DOI: 10.1039/d1cs01114f.

(10) Sahu, A.; Mahapatra, S.; Dey, P.; Ghosh, G. Harnessing Crystallization-Driven Self-Assembly (CDSA) of Semicrystalline Block Copolymers for Functional 2D Architectures and Their Applications. *Macromolecular Chemistry and Physics* **2025**. DOI: 10.1002/macp.202400426.

(11) Zhang, J.; Cao, H.; Wan, X.; Zhou, Q. Molecular Reorganization of Rod−Coil Diblock Copolymers at the Air−Water Interface. *Langmuir* **2006**, *22* (15), 6587-6592. DOI: 10.1021/la060844h.

(12) Zhang, J.; Lin, W.; Liu, A.; Yu, Z.; Wan, X.; Liang, D.; Zhou, Q. Solvent Effect on the Aggregation Behavior of Rod−Coil Diblock Copolymers. *Langmuir* **2008**, *24* (8), 3780-3786. DOI: 10.1021/la703888m.

(13) Gao, L.; Gao, H.; Lin, J.; Wang, L.; Wang, X.-S.; Yang, C.; Lin, S. Growth and Termination of Cylindrical Micelles via Liquid-Crystallization-Driven Self-Assembly. *Macromolecules* **2020**, *53* (20), 8992-8999. DOI: 10.1021/acs.macromol.0c01820.

(14) Lin, X.; He, X.; Hu, C.; Chen, Y.; Mai, Y.; Lin, S. Disk-like micelles with cylindrical pores from amphiphilic polypeptide block copolymers. *Polymer Chemistry* **2016**, *7* (16), 2815-2820. DOI: 10.1039/c6py00152a.

(15) Jin, X.; Wu, F.; Lin, J.; Cai, C.; Wang, L.; Chen, J.; Gao, L. Programmable Morphology Evolution of Rod-Coil-Rod Block Copolymer Assemblies Induced by Variation of Chain Ordering. *Langmuir* **2021**, *37* (10), 3148-3157. DOI: 10.1021/acs.langmuir.0c03644.

(16) Stupp, S. I. Self-assembly of rodcoil molecules. *Current Opinion in Colloid & Interface Science* **1998**, *3* (1), 20-26. DOI: https://doi.org/10.1016/S1359-0294(98)80037-X.

(17) Contini, C.; Pearson, R.; Wang, L.; Messager, L.; Gaitzsch, J.; Rizzello, L.; Ruiz-Perez, L.; Battaglia, G. Bottom-Up Evolution of Vesicles from Disks to High-Genus Polymersomes. *iScience* **2018**, *7*, 132-144. DOI: 10.1016/j.isci.2018.08.018.

(18) Qiao, S.; Li, S.; Song, Q.; Liu, B. Shape-Tunable Biconcave Disc-Like Polymer Particles by Swelling-Induced Phase Separation of Seeded Particles with Hydrophilic Shells. *Langmuir* **2023**, *39* (3), 1190-1197. DOI: 10.1021/acs.langmuir.2c02995.

(19) Thiermann, R.; Bleul, R.; Maskos, M. Kinetic Control of Block Copolymer Self-Assembly in a Micromixing Device – Mechanistical Insight into Vesicle Formation Process. *Macromolecular Chemistry and Physics* **2017**, *218* (2), 1600347. DOI: 10.1002/macp.201600347.

(20) Jia, F.; Liang, F.; Yang, Z. Janus Mesoporous Nanodisc from Gelable Triblock Copolymer. *ACS Macro Letters* **2016**, *5* (12), 1344-1347. DOI: 10.1021/acsmacrolett.6b00812.

(21) Li, Z.; Chen, Z.; Cui, H.; Hales, K.; Qi, K.; Wooley, K. L.; Pochan, D. J. Disk Morphology and Disk-to-Cylinder Tunability of Poly(Acrylic Acid)-b-Poly(Methyl Acrylate)-b-Polystyrene Triblock Copolymer Solution-State Assemblies. *Langmuir* **2005**, *21* (16), 7533-7539. DOI: 10.1021/la051020n.

(22) Zhu, J.; Zhang, S.; Zhang, K.; Wang, X.; Mays, J. W.; Wooley, K. L.; Pochan, D. J. Disk-cylinder and disk-sphere nanoparticles via a block copolymer blend solution construction. *Nature Communications* **2013**, *4* (1). DOI: 10.1038/ncomms3297.

(23) Shi, Y.; Zhu, W.; Yao, D.; Long, M.; Peng, B.; Zhang, K.; Chen, Y. Disk-Like Micelles with a Highly Ordered Pattern from Molecular Bottlebrushes. *ACS Macro Letters* **2014**, *3* (1), 70-73. DOI: 10.1021/mz400619g.

(24) Zeng, H.; Liang, X.; Roberts, D. A.; Gillies, E. R.; Müllner, M. Self-Assembly of Rod-Coil Bottlebrush Copolymers into Degradable Nanodiscs with a UV-Triggered Self-Immolation Process. *Angewandte Chemie International Edition* **2024**, *63* (13). DOI: 10.1002/anie.202318881.

(25) Zeng, H.; Zeng, P.; Baek, J.; Kim, B. S.; Müllner, M. Self-Assembly of Amorphous 2D Polymer Nanodiscs with Tuneable Size, pH-Responsive Degradation and Controlled Drug Release. *Angewandte Chemie International Edition* **2025**. DOI: 10.1002/anie.202424269.

(26) Zheng, Z.; Müllner, M.; Ling, J.; Müller, A. H. E. Surface Interactions Surpass Carbon–Carbon Bond: Understanding and Control of the Scission Behavior of Core–Shell Polymer Brushes on Surfaces. *ACS Nano* **2013**, *7* (3), 2284-2291. DOI: 10.1021/nn3054347.

(27) Neugebauer, D.; Sumerlin, B. S.; Matyjaszewski, K.; Goodhart, B.; Sheiko, S. S. How dense are cylindrical brushes grafted from a multifunctional macroinitiator? *Polymer* **2004**, *45* (24), 8173-8179. DOI: https://doi.org/10.1016/j.polymer.2004.09.069.

(28) Yoshikawa, C.; Sakakibara, K.; Nonsuwan, P.; Yamazaki, T.; Tsujii, Y. Nonbiofouling Coatings Using Bottlebrushes with Concentrated Polymer Brush Architecture. *Biomacromolecules* **2021**, *22* (6), 2505-2514. DOI: 10.1021/acs.biomac.1c00247.

(29) Takano, S.; Nishimura, T.; Cheng, Y. T.; Müllner, M. Self-Assembly of Thioether-Based Diblock Copolymers: A Comparative Study of Linear and Bottlebrush Architectures. *Polymer Chemistry* **2025**. DOI: 10.1039/d5py00153f.

(30) Hou, W.; Wu, J.; Li, Z.; Zhang, Z.; Shi, Y.; Chen, Y. Efficient Synthesis and PISA Behavior of Molecular Bottlebrush Block Copolymers via a Grafting-From Strategy through RAFT Dispersion Polymerization. *Macromolecules* **2023**, *56* (3), 824-832. DOI: 10.1021/acs.macromol.2c02233.

(31) Birshtein, T. M.; Borisov, O. V.; Zhulina, Y. B.; Khokhlov, A. R.; Yurasova, T. A. Conformations of comb-like macromolecules. *Polymer Science U.S.S.R.* **1987**, *29* (6), 1293-1300. DOI: https://doi.org/10.1016/0032-3950(87)90374-1.

(32) Modica, K. J.; Martin, T. B.; Jayaraman, A. Effect of Polymer Architecture on the Structure and Interactions of Polymer Grafted Particles: Theory and Simulations. *Macromolecules* **2017**, *50* (12), 4854-4866. DOI: 10.1021/acs.macromol.7b00524.

(33) Theodorakis, P. E.; Hsu, H.-P.; Paul, W.; Binder, K. Computer simulation of bottle-brush polymers with flexible backbone: Good solvent versus theta solvent conditions. *The Journal of Chemical Physics* **2011**, *135* (16), 164903. DOI: 10.1063/1.3656072.

(34) Qi, M.; Zhou, Y. Multimicelle aggregate mechanism for spherical multimolecular micelles: from theories, characteristics and properties to applications. *Materials Chemistry Frontiers* **2019**, *3* (10), 1994-2009. DOI: 10.1039/c9qm00442d.

(35) Bolisetty, S.; Airaud, C.; Xu, Y.; Müller, A. H. E.; Harnau, L.; Rosenfeldt, S.; Lindner, P.; Ballauff, M. Softening of the stiffness of bottle-brush polymers by mutual interaction. *Physical Review E* **2007**, *75* (4). DOI: 10.1103/physreve.75.040803.

(36) Lin, T.-P.; Chang, A. B.; Luo, S.-X. L.; Chen, H.-Y.; Lee, B.; Grubbs, R. H. Effects of Grafting Density on Block Polymer Self-Assembly: From Linear to Bottlebrush. *ACS Nano* **2017**, *11* (11), 11632-11641. DOI: 10.1021/acsnano.7b06664.

(37) Hsu, H.-P.; Paul, W.; Rathgeber, S.; Binder, K. Characteristic Length Scales and Radial Monomer Density Profiles of Molecular Bottle-Brushes: Simulation and Experiment. *Macromolecules* **2010**, *43* (3), 1592-1601. DOI: 10.1021/ma902101n.

(38) Zhulina, E. B.; Sheiko, S. S.; Borisov, O. V. Theoretical advances in molecular bottlebrushes and comblike (co)polymers: solutions, gels, and self-assembly. *Soft Matter* **2022**, *18* (46), 8714-8732. DOI: 10.1039/d2sm01141g.

(39) Zhang, H.; Diesendruck, C. E. Linear versus Helical Side Chains in Bottlebrush Polymers: Morphology and Mechanochemistry. *Macromolecules* **2024**, *57* (8), 3664-3670. DOI: 10.1021/acs.macromol.3c02573.

(40) Sunday, D. F.; Burns, A. B.; Martin, T. B.; Chang, A. B.; Grubbs, R. H. Relationship between Graft Density and the Dilute Solution Structure of Bottlebrush Polymers: An Inter-chemistry Comparison and Scaling Analysis. *Macromolecules* **2023**, *56* (18), 7419-7431. DOI: 10.1021/acs.macromol.3c01436.

(41) Ulrich, H. F.; Gruschwitz, F. V.; Klein, T.; Ziegenbalg, N.; Anh, D. T. N.; Fujii, S.; Hoeppener, S.; Sakurai, K.; Brendel, J. C. Influence of Polymer Side Chain Size and Backbone Length on the Self-Assembly of Supramolecular Polymer Bottlebrushes. *Chemistry – A European Journal* **2024**, *30* (26). DOI: 10.1002/chem.202400160.

(42) Panyukov, S.; Zhulina, E. B.; Sheiko, S. S.; Randall, G. C.; Brock, J.; Rubinstein, M. Tension Amplification in Molecular Brushes in Solutions and on Substrates. *The Journal of Physical Chemistry B* **2009**, *113* (12), 3750-3768. DOI: 10.1021/jp807671b.

(43) Pan, X.; Ding, M.; Li, L. Experimental Validation on Average Conformation of a Comblike Polystyrene Library in Dilute Solutions: Universal Scaling Laws and Abnormal SEC Elution Behavior. *Macromolecules* **2021**, *54* (23), 11019-11031. DOI: 10.1021/acs.macromol.1c01029.

(44) Xiao, L.; Li, J.; Peng, G.; Huang, G. The effect of grafting density and side chain length on the conformation of PEG grafted bottlebrush polymers. *Reactive and Functional Polymers* **2020**, *156*, 104736. DOI: https://doi.org/10.1016/j.reactfunctpolym.2020.104736.

(45) Doi, N.; Yamauchi, Y.; Sasai, Y.; Yuda, N.; Kuzuya, M.; Kondo, S. I. Characterization of well-defined <scp>PHEMA</scp>-based bottlebrushes with controlled chain length and grafting density. *Journal of Polymer Science* **2024**, *62* (7), 1310-1322. DOI: 10.1002/pol.20230653.

(46) Christie, D.; Register, R. A.; Priestley, R. D. Direct Measurement of the Local Glass Transition in Self-Assembled Copolymers with Nanometer Resolution. *ACS Central Science* **2018**, *4* (4), 504-511. DOI: 10.1021/acscentsci.8b00043.

(47) Kaya, İ.; Pala, Ç. Y. Thermodynamics of poly(benzyl methacrylate)–probe interactions at different temperatures by using inverse gas chromatography. *Fluid Phase Equilibria* **2014**, *374*, 63-69. DOI: https://doi.org/10.1016/j.fluid.2014.04.005.

(48) Burel, F.; Rossignol, L.; Pontvianne, P.; Hartman, J.; Couesnon, N.; Bunel, C. Synthesis and characterization of poly(ethyl glyoxylate) – a new potentially biodegradable polymer. *e-Polymers* **2003**, *3* (1). DOI: 10.1515/epoly.2003.3.1.407.

(49) Song, J.; Hwang, E.; Lee, Y.; Palanikumar, L.; Choi, S.-H.; Ryu, J.-H.; Kim, B.-S. Tailorable degradation of pH-responsive all polyether micelles via copolymerisation with varying acetal groups. *Polymer Chemistry* **2019**, *10* (5), 582-592. DOI: 10.1039/c8py01577e.

(50) Zhuang, Z.; Cai, C.; Jiang, T.; Lin, J.; Yang, C. Self-assembly behavior of rod–coil–rod polypeptide block copolymers. *Polymer* **2014**, *55* (2), 602-610. DOI: https://doi.org/10.1016/j.polymer.2013.12.016.

(51) Liberman, L.; Coughlin, M. L.; Weigand, S.; Edmund, J.; Bates, F. S.; Lodge, T. P. Impact of Side-Chain Length on the Self-Assembly of Linear-Bottlebrush Diblock Copolymers. *Macromolecules* **2022**, *55* (12), 4947-4955. DOI: 10.1021/acs.macromol.2c00758.

(52) Vu, C.; Abu Amara, N.; Alaboalirat, M.; Nativ-Roth, E.; Zalk, R.; Leite, W.; Carrillo, J.-M.; Bitton, R.; Matson, J. Aqueous self-assembly of cylindrical and tapered bottlebrush block copolymers. American Chemical Society (ACS): 2024.

(53) Mikhailov, I. V.; Zhulina, E. B.; Borisov, O. V.; Nardin, C.; Darinskii, A. A. Architectural control over morphologies of bottlebrush block copolymer superstructures. *AIP Advances* **2023**, *13* (12). DOI: 10.1063/5.0179466.

(54) Sánchez-Leija, R. J.; Mysona, J. A.; De Pablo, J. J.; Nealey, P. F. Phase Behavior and Conformational Asymmetry near the Comb-to-Bottlebrush Transition in Linear-Brush Block Copolymers. *Macromolecules* **2024**, *57* (5), 2019-2029. DOI: 10.1021/acs.macromol.3c02180.

(55) Perales Rodriguez, C.; Mahanthappa, M. K.; Lodge, T. P. Lyotropic Phase Behavior of Coil-Bottlebrush Diblock Copolymers in Alkylimidazolium-Based Ionic Liquids. *Macromolecules* **2024**, *57* (7), 3081-3089. DOI: 10.1021/acs.macromol.3c02451.

(56) Zhang, J.; Song, Q.; Peng, L.; Huang, X.; Li, W. Square Array of Cylinders Formed in Linear–Bottlebrush–Linear Triblock Copolymers. *Macromolecules* **2025**, *58* (8), 4112-4121. DOI: 10.1021/acs.macromol.5c00357.

(57) Lebedeva, I. O.; Zhulina, E. B.; Borisov, O. V. Self-Assembly of Bottlebrush Block Copolymers in Selective Solvent: Micellar Structures. *Polymers* **2021**, *13* (9), 1351. DOI: 10.3390/polym13091351.